

A New Perspective in Groundwater Flow Modelling - Application of Lagging Theory

Ying-Fan Lin¹, Ali Mahdavi², and Tung-Chou Hsieh³

¹National Taiwan University

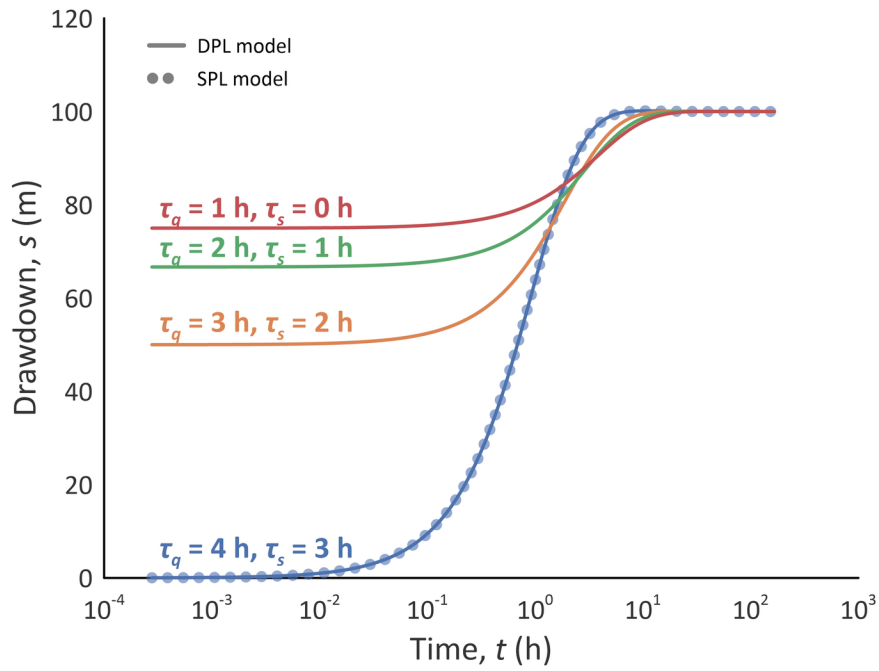
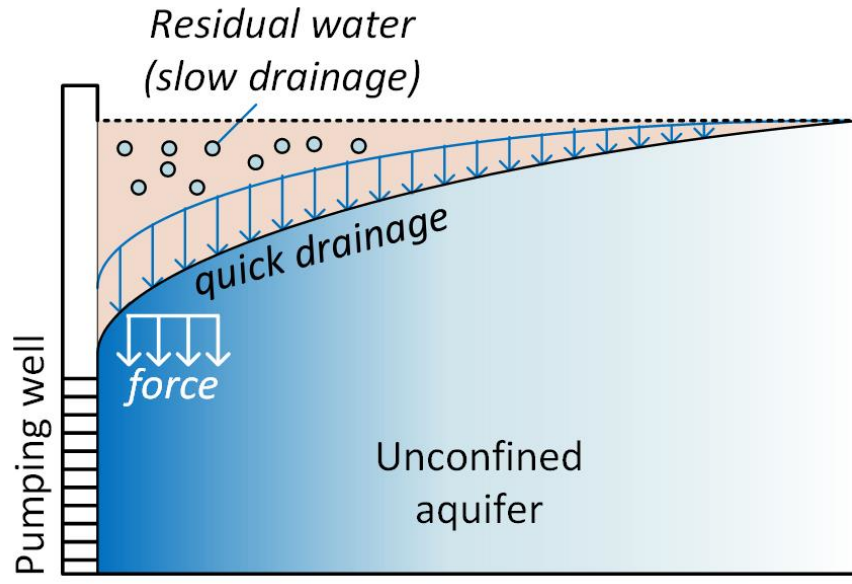
²Arak University

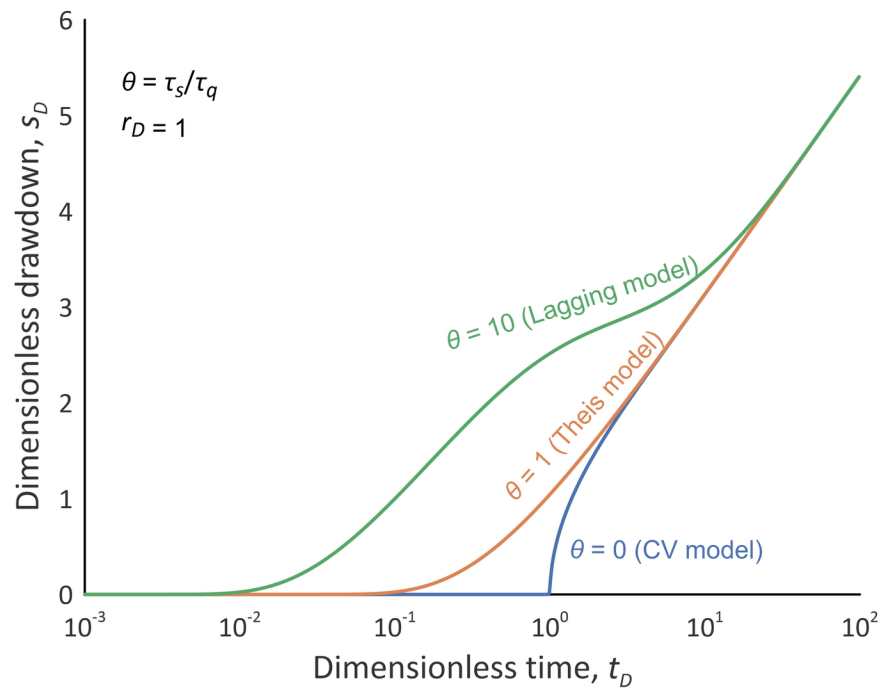
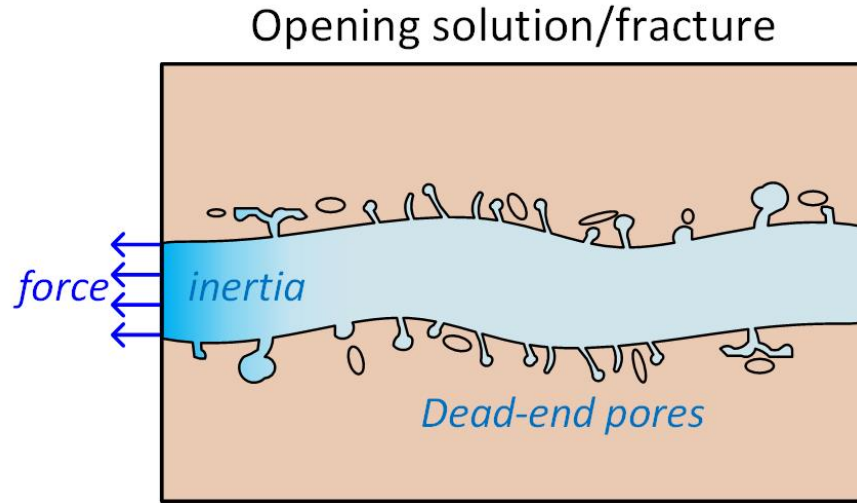
³Disaster Prevention and Water Environment Research Center, National Yang Ming Chiao Tung University

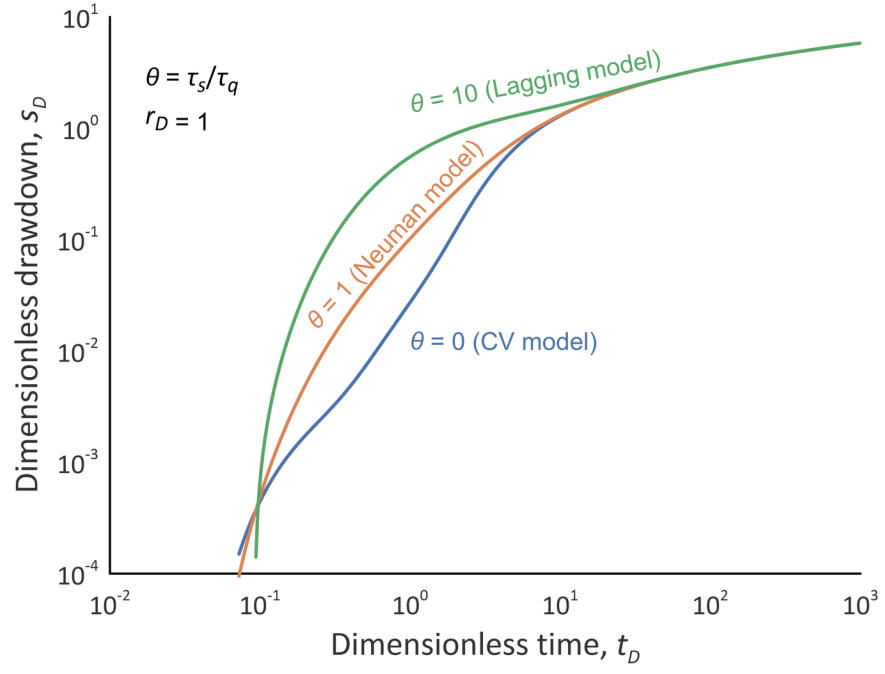
November 22, 2022

Abstract

Lagging theory has emerged to construct mathematical models to describe groundwater flow since 2017 due to the addition of two lagging parameters to simply represent a complex physical model; however, the original theory, called *dual-phase lag* theory, has been widely applied to heat transfer problems since 1995. As yet, lagging theory has already been applied to develop the mathematical model related to well hydraulic in confined or unconfined aquifers and stream depletion prediction problems. For example, the effects of water inertia, dead-end or small-pore storage, capillary fringe exceeding storage, capillary suction, and streambed storage on the hydraulic response can all be simply represented by two lagging parameters, whereas the physical-based model may necessitate more in situ measures as inputs to the model. Although it has some benefits for data interpretation, there are only a few studies (merely five published papers) that specifically focus on the application of lagging theory to the problem of groundwater flow because the physical meaning of lagging parameters remains somewhat unclear. This study aims to present a brief review of studies on groundwater flow problems and to discuss the physical insights behind the concept of lagging theory. The threshold value analysis is used to investigate the lagging effect on the drawdown. In addition, we introduce several candidate models regarding the hydrology or well hydraulic for future research directions.







Abstract

Lagging theory has emerged to construct mathematical models to describe groundwater flow since 2017 due to the addition of two lagging parameters to simply represent a complex physical model; however, the original theory, called *dual-phase lag theory*, has been widely applied to heat transfer problems since 1995. As yet, lagging theory has already been applied to develop the mathematical model related to well hydraulic in confined or unconfined aquifers and stream depletion prediction problems. For example, the effects of water inertia, dead-end or small-pore storage, capillary fringe exceeding storage, capillary suction, and streambed storage on the hydraulic response can all be simply represented by two lagging parameters, whereas the physical-based model may necessitate more in situ measures as inputs to the model. Although it has some benefits for data interpretation, there are only a few studies (merely five published papers) that specifically focus on the application of lagging theory to the problem of groundwater flow because the physical meaning of lagging parameters remains somewhat unclear. This study aims to present a brief review of studies on groundwater flow problems and to discuss the physical insights behind the concept of lagging theory. The threshold value analysis is used to investigate the lagging effect on the drawdown. In addition, we introduce several candidate models regarding the hydrology or well hydraulic for future research directions.

Keywords *Lagging theory, Dual-phase lag model, Well hydraulic, Analytical model*

1 Introduction

1.1 Background

Groundwater is a vital water resource in many areas to supply the growth of plants and living organisms and satisfy human demand for industrial use and artificial irrigation. To utilize groundwater, drilling a pumping well is common to extract groundwater from the aquifer. Knowing the mechanism of groundwater flow facilitates the development of a sound strategy for the management of water resources. Therefore, well hydraulics has become one of the promising studies in contemporary hydrology. However, accurately predicting groundwater flow motion is a challenging task if data are taken from limited observation stations. To cope with these problems, mathematical models have been developed to depict groundwater flow derived from an empirical constitutive relation coupled with physical laws. For the groundwater flow problem, the constitutive relation usually refers to Darcy's law, whereas the physical laws include the continuity equation and initial/boundary conditions. The methods for solving groundwater flow equations fall into two main groups — the analytical method and the numerical method. Analytical methods often include integral transformation methods (e.g., Laplace transform, Fourier transform, Hankel transform, etc.), the change of variable method, and separation of variables method. On the other hand, numerical methods

46 may contain the finite difference method, finite element method, finite volume method, or meshless
 47 method (sometimes the meshless method is left outside of the category of numerical method). Both
 48 analytical and numerical methods have successfully solved groundwater flow equations depending
 49 on the conditions and problems of the model.

50 1.2 Basic Flow Equation for Pumping Problem

51 According to the continuity condition, the groundwater flow equation in three-dimensional (3D)
 52 Cartesian coordinates considering a fully penetrating well in a confined aquifer can be expressed as

$$S_s \frac{\partial s}{\partial t} - \frac{Q}{b} \delta(x - x_0) \delta(y - y_0) = -\nabla \mathbf{q} \quad (1)$$

53 where S_s is the specific storage [L^{-1}], s is the drawdown (the change in water level) [L], t is the time,
 54 (x, y) is the Cartesian location, (x_0, y_0) is the pumping well location, b is the aquifer thickness, δ
 55 is the Dirac delta function, and \mathbf{q} is the tensor of the specific flux [LT^{-1}]. Darcy's law says that the
 56 water flux is linearly proportional to the hydraulic gradient, meaning that

$$\mathbf{q} = -\mathbf{K} \nabla s \quad (2)$$

57 where \mathbf{K} is the tensor of the hydraulic conductivity [LT^{-1}]. Inserting equation (2) into (1), one can
 58 obtain a 3D groundwater flow model for the pumping problem:

$$S_s \frac{\partial s}{\partial t} - \frac{Q}{b} \delta(x - x_0) \delta(y - y_0) = K_x \frac{\partial^2 s}{\partial x^2} + K_y \frac{\partial^2 s}{\partial y^2} + K_z \frac{\partial^2 s}{\partial z^2} \quad (3)$$

59 For polar coordinates, it gives

$$S_s \frac{\partial s}{\partial t} - \frac{Q}{r\pi b} \delta(r - r_0) \delta(\theta - \theta_0) = K_r \frac{1}{r} \frac{\partial}{\partial r} \left(r \frac{\partial s}{\partial r} \right) + K_\theta \frac{1}{r^2} \frac{\partial^2 s}{\partial \theta^2} \quad (4)$$

60 in which r is the radial direction [L], θ is the angle, and (r_0, θ_0) is the pumping well location.

61 For the problem of the aquifer pumping test, the flow equation is generally considered an
 62 isotropic aquifer (in the θ direction). The pumping source (point source) is often imposed on the
 63 inner boundary (line source) but not in the governing equation. Thus, the governing equation and
 64 the pumping-related boundary condition are, respectively, given as

$$S_s \frac{\partial s}{\partial t} = K_r \frac{1}{r} \frac{\partial}{\partial r} \left(r \frac{\partial s}{\partial r} \right) \quad (5)$$

65 and

$$2\pi K_r b \lim_{r \rightarrow 0} r \frac{\partial s}{\partial r} = -Q \quad (6)$$

66 1.3 Origin of Lagging Theory

67 The Darcy law provides a starting point to illustrate the lagging theory. As mentioned above,
 68 the Darcy law describes a linear relationship between the specific flux and the drawdown gradient.

69 This finding is quite useful for building a groundwater flow model if the law is coupled with the
 70 continuity equation. On the other hand, the fundamental concept of *lagging theory* is to assume
 71 that there exist time delays in the Darcy law. The lagging theory is originally derived from the idea
 72 of the concept of *dual-phase lag* (DPL) proposed by the forerunner *Tzou* [1995] for the nonlinear
 73 Fourier law by placing two lagging parameters individually in the heat flux and thermal gradient to
 74 interpret the effects of the thermal inertia and microstructural interactions observed in short-pulse
 75 laser experiments. The experiments demonstrated an oscillatory behavior (thermal wave) of temporal
 76 temperature curves, implying that the heat transfer speed is finite. The DPL can be viewed as an
 77 advance in the Cattaneo-Vernotte (CV) model [Cattaneo, 1958; Vernotte, 1958, 1961], which only
 78 considered one lagging parameter in the flux term of the Fourier law; namely, the CV model is a
 79 single-phase lag model (SPL).

80 The DPL concept was not only subsequently applied to the heat conduction problems induced
 81 by rapid laser pulses, but was also used to study the mass transport for silicon dioxide film growth
 82 (Fick's first law), thermoelectricity, thermoelastic deformation, viscothermoelastic response, heat
 83 transfer in nanofluids, and bioheat response [Tzou, 1995]. Google Scholar search results using the
 84 keywords "dual-phase lag" will provide a total of 357,000 search results (searched on 10^{ed} August
 85 2022). This means that DPL models are still in rapid development to study the thermal response in
 86 the thermal engineering community today. Furthermore, it can be seen from the cloud word resulting
 87 from Google Scholar shown in Figure 1, that the DPL model is applied mainly to studies of heat
 88 conduction problems and mass transport problems. However, research on the application of the DPL
 89 concept to the groundwater field has been reported in: *Lin and Yeh* [2017], *Lin et al.* [2019], *Huang*
 90 *et al.* [2020], *Xiong et al.* [2021], and *Sarmah et al.* [2022]. In total, four articles have been published
 91 in *Water Resources Research* and one in *Hydrological Sciences Journal*. Notice that the last three
 92 studies developed the boundary condition based on SPL or CV.

93 Here, we would like to focus our attention on the concepts between the lagging theory and the
 94 DPL theory. Obviously, two models are developed on the basis of the same concept. However, as
 95 can be seen in Figure 1, people will naturally link the DPL model to the heat transfer problem when
 96 looking for DPL-related studies. To address this problem, we particularly use the term lagging theory
 97 for the groundwater flow model rather than the DPL model. Lagging theory particularly refers to the
 98 Darcy law that includes lag times and is defined as the specific discharge and the drawdown gradient
 99 which occur at two different times, giving rise to the following.

$$\mathbf{q}(t + \tau_q) = -\mathbf{K}\nabla s(t + \tau_s) \quad (7)$$

100 wherein τ_q and τ_s [T] are the lagging parameters. If $\tau_s = 0$, it becomes a CV/SLP-based law:

$$\mathbf{q}(t + \tau) = -\mathbf{K}\nabla s(t) \quad (8)$$

101 where τ is the relaxation time [L] for the CV/SLP model.

There are three important properties of the lagging time parameters τ_q and τ_s :

1. When $\tau_q > \tau_s$, it means that the drawdown gradient is the cause and the specific flux is the result of the flux. In this case, the time drawdown curve with time on a logarithmic scale shows a gradually increasing drawdown value with time.
2. When $\tau_q < \tau_s$, it means that the flux is the cause and the drawdown gradient is the result. The time-drawdown curve in the semi-lag graph will exhibit an S-shaped pattern.
3. If $\tau_q = \tau_s$, the flux and gradient occur instantaneously ($\tau_q = \tau_s = 0$); in this case, the lagging Darcy law is equivalent to the classical one, and the drawdown curve will be similar to the curve yield by the conventional confined flow model. Three cases are schematically represented in Figure 2.

In addition, the Darcy law with lagging effects coupled with the continuity equation for the aquifer will result in Jeffery's equation. This means that the drawdown (energy) propagation speed is changed from infinite (diffusion/heat equation) to finite.

1.4 Objective of the Work

The main objective of this work is to review the paper related to lagging theory and continue to reconnect the link between the lagging theory and the DPL concept. The use of the term "lagging theory" may cause the reader to forget where it came from. Moreover, to further explore the applicability of the lagging theory, this study hopes to find more applications to hydrology to guide more follow-up studies.

2 Analytical Framework in Well Hydraulic

2.1 Pumping in Fractured Aquifer

Having defined the lagging theory in Section 1.3, we can focus our attention on the literature review related to the lagging theory. In the twentieth century, two mathematical models for groundwater flow have been developed by *Pascal* [1986] and *Löfqvist and Rehbinder* [1993] to include the effect of water inertia due to pumping by adding a relaxation time. It results in a

The governing equations of their models are more like the CV/SPL model; therefore, their studies are more concentrated on the effect of the inertial force on the groundwater flow response.

However, the first paper on lagging theory (i.e., using the DPL concept) was presented by *Lin and Yeh* [2017]. They applied lagging theory to the mathematical model to describe the drawdown s due to pumping situated in a leaky fractured aquifer. Two lagging parameters τ_q and τ_s were included in the Darcy law to reflect the effects of water inertia due to the high velocity of the flow

and the microstructural interactions resulting from the release of water from dead-end pores or very small pores, respectively. These two effects are related to the higher pump-induced water speed in the fractures and opening solutions and the mass transfer between two overlapped fractured and matrix continua, respectively (see Figure 3). In combination with the continuity equation for the aquifer system, the governing equation of the groundwater flow based on lagging theory is a type of wave equation. Consequently, the infinite drawdown propagation speed (for a classical groundwater equation, a diffusion/heat equation) becomes finite. The time-drawdown curve predicted by the *Lin and Yeh* [2017] solution shows an S-shaped pattern, which is the standard feature of the pump-induced drawdown curve for unconfined flow [*Neuman*, 1975a] and DP flow [*Warren and Root*, 1963; *Chaudhry*, 2003]. *Lin and Yeh* [2017] demonstrated that their model is similar to the DP model, although the latter cannot reflect the inertial effect because some of its hydraulic parameters bear some nonnegative properties. The relations are shown as

$$\tau_q = \frac{S_m S_f}{\beta(S_f + S_m)} \quad (9)$$

$$\tau_s = \frac{S_m}{\beta} \quad (10)$$

129 where the subscripts f and m represent the fracture and matrix, respectively, $\beta = K_m \sigma$ with the
 130 hydraulic conductivity of the matrix K_m [LT^{-1}] and the water transfer coefficient σ [T^{-1}]. Equation
 131 (9) shows the physical information of the lagging parameters. Apparently, τ_q in this model is the
 132 result of secondary pores storage. However, an interesting finding from their work on changing
 133 values of lagging parameters is that the parameters appear to affect the time when the additional
 134 water begins to recharge the well and stops to do so. This feature of the lagging effects is helpful
 135 for parameter identification to provide proper initial guesses for the lagging parameters when we
 136 are trying to fit an S-shaped drawdown curve. Although there is a similarity between the lagging
 137 confined aquifer model and the dual porosity (DP) model, equation (9) implies $\tau_q \leq \tau_s$ for the
 138 DP model that may fail to predict the groundwater flow dominated by inertial forces. Yet, if the
 139 drawdown curves show an S-shaped pattern presented in a semi-log graph, one can know that τ_s
 140 must be greater than τ_q ; therefore, equation (9) can be used to determine the initial values of lagging
 141 parameters.

142 In terms of identification of hydraulic parameters, *Lin and Yeh* [2017] applied their confined
 143 leaky solution coupled lagging theory to analyze the time-drawdown curves observed in five observa-
 144 tion wells of the pumping test conducted by *Greene* [1993] in the Madison fractured aquifer. Accord-
 145 ing to their estimated results, the lagging time parameters may be in the range of $\tau_q \in [0.089, 13.95]$
 146 and $\tau_s \in [0.05, 7.1]$ hour units. It is particularly relevant for the Madison aquifer, but can be used as
 147 reference values or as a constraint when performing a parameter estimation for a fractured aquifer.

2.2 Pumping in Unconfined Aquifer

Instead of applying the lagging theory to the Darcy law governing an aquifer, the theory can also be utilized to describe the vertical water flux above the water table in an unconfined aquifer system. *Lin et al.* [2019] attempted to apply the lagging theory to the kinematic condition of the water table, which describes the drainage from the unsaturated soils above once the water table declined. This work may be the first attempt to use the lagging theory (DPL concept) to a boundary condition only. The pump-induced unconfined flow features its S-shaped time-drawdown curve, where the flattening portion of the curve results from gravity drainage. This phenomenon is called delayed drainage, and its effect is evaluated by the dimensionless parameter, the specific yield S_y [-]. To show this effect, many models for pump-induced unconfined flow were developed considering a source term in the flow equation [Boulton, 1954a], using a kinematic condition at the water table [Boulton, 1954b; Neuman, 1972, 1974, 1975b; Moench, 1995; Malama, 2011], and accounting for the unsaturated zone above the water table [Mathias and Butler, 2006; Tartakovsky and Neuman, 2007; Mishra and Neuman, 2010]. These models are successful in fitting the field drawdown data and significantly improve the estimate of S_y . Compared to these models, the benefit of using kinematic condition at the water table makes the model simple and only one governing equation is required to be solved. The main improvement of the model of *Lin et al.* [2019] is that they considered the flow in the z (vertical) direction, q_z , and the hydraulic gradient, $K_z \partial s / \partial z$, at the water table to occur at different times, say $q_z(t + \tau_q) = K_z \partial s(t + \tau_s) / \partial z$. Thus, delayed drainage can emerge at early times (in classical theory, aquifer storage should prevail over delayed drainage) and prolong its effect at late times; both reflect the effects of excess capillary storage dragged by pumping and capillary suction holding the residual pore water, respectively (see Figure 4). More specifically, the lagging time parameter τ_q plays a role in reflecting the rapid drainage dragged from the exceed capillary storage due to the higher rate of decrease of the water table near a pumping well. The parameter τ_s represents the residual storage on the capillary fringe after the water table is moved downwards and then gradually recharges to the aquifer. Similar findings are also reported in *Nwankwor et al.* [1992] and *Bevan et al.* [2005]. The results of parameter identification in *Lin et al.* [2019] revealed that the estimates of τ_q and τ_s decrease with increasing observation distance from the test well. It is so because the effects of lagging parameters become immaterial ($\tau_q \approx 0$ and $\tau_s \approx 0$) when the pumping well is too far away to have a significant influence on the vertical groundwater flow. Moreover, *Lin et al.* [2019] showed that if τ_q equals zero, the lagging water table kinematic condition will reduce to the *Moench* [1995] condition, which was derived for noninstantaneous drainage due to the unsaturated flux. In addition, *Lin et al.* [2019] analyzed the unconfined drawdown data from four observation wells in Cape Cod, Massachusetts [Moench et al., 2000], four wells in the Borden Canadian Forces Base, Canada [Bevan et al., 2005], and two wells in Saint Pardon de Conques, Gironde, France [Neuman, 1975b], to estimate the hydraulic parameters, including lagging time parameters. We concluded that the possible range of lagging parameters τ_q and τ_s would be in the range of $\tau_q \in [0.67, 194.37]$ and

185 $\tau_s \in [30.37, 469.40]$ hour unit. These ranges for unconfined aquifers are quite larger than those in
 186 a confined aquifer. In summary, the possible ranges of the lagging parameters for fractured aquifer
 187 and unconfined aquifer are listed in Table 1. The value of the threshold value $\theta = \tau_s/\tau_q$ listed in the
 188 table also help to reveal what mechanic dominates the flow system. The detailed analysis of θ will
 189 be postponed to Section 2.1 due to the dimensionless analysis involved.

190 2.3 Pumping near a Stream

191 For the pump-induced stream depletion problem, *Huang et al.* [2020] adopted the concept of
 192 the lagging theory to reflect the time lag of the water flow from a river on account of the streambed
 193 storage, which can retard the flow of water to the pumping well. Such a treatment has the benefit of
 194 reducing the model complexity; for example, the streambed flow equation is replaced by a Robin-
 195 type boundary condition with a lagging effect. The original Robin-type condition at the interface
 196 between the stream and the pumped aquifer can be expressed as $q(t) = -K\partial s(t)/\partial x$, where x is
 197 the direction from the pumping well to the stream [L]. Taking into account first-order mass transfer,
 198 q can be written as $\beta(0 - s)$, where β is the conductance of the streambed [T^{-1}]. The difference
 199 is that their model considered one lagging parameter in terms of q . This treatment is more like an
 200 SPL model as mentioned previously, which can be viewed as a special case of the DPL model. *Tzou*
 201 [1995] indicated that the use of the SLP model may fail to describe the slow thermalization process
 202 because its inherent in the precedence of the gradient over the flux. *Huang et al.* [2020] tried to
 203 connect the lag time parameter τ and the property of the stream bed by applying the final value
 204 theorem to its Laplace domain solution, and found that τ is equivalent to $w^2 S'_s / K'$, wherein w is the
 205 width of the streambed [L] and S'_s and K' are the specific storage [L^{-1}] and hydraulic conductivity
 206 [TL^{-1}] of the streambed, respectively. Furthermore, Huang and his colleagues [*Xiong et al.*, 2021]
 207 modified the existing models for pump-induced stream depletion, including the works of *Spalding*
 208 *and Khaleel* [1991], *Sophocleous et al.* [1995], *Hunt* [1999], *Hunt* [1999], and *Sun and Zhan* [2007],
 209 by adding the SPL-like or CV-like boundary condition. One can note that the consideration of a
 210 lagging time parameter representing the streambed effect may not significantly improve the result
 211 of parameter estimation according to the values of the standard error of the estimate in Table 3 of
 212 their work. This is because the storage of the streambed merely yields a small value of drawdown or
 213 stream depletion, whereupon its impact on the inverse problem becomes minor. To cope with this
 214 problem, early time measurements should be monitored more frequently. Otherwise, the weights
 215 of the hydraulic response at intermediate and late times would prevail over the estimated results for
 216 parameter identification. The other reason is that the DPL and SPL assumptions are mathematically
 217 different, although the DPL model $q(t + \tau_q) = \mathbf{K}\nabla s(t + \tau_s)$ appears to be reduced to the SPL model
 218 by subtracting τ_s from both sides: $q(t + \tau_q - \tau_s) = \mathbf{K}\nabla s(t)$.

3 Methodology

3.1 Threshold Value Analysis

3.1.1 Confined Flow

Of particular interest is the threshold value θ , defined as τ_s/τ_q , which can characterize the effects of τ_q and τ_s . The effect of θ has not been discussed in previous studies. Here, the model of *Lin and Yeh* [2017] will be applied to evaluate the effect of θ , but for simplicity, the effects of the wellbore storage and the aquitard leakage are neglected. The new dimensionless parameters and variables are defined as

$$s_D = \frac{4\pi T s}{Q}, \quad r_D = \frac{r}{\sqrt{T\tau_q/S}}, \quad r_{w,D} = \frac{r_w}{\sqrt{T\tau_q/S}}, \quad t_D = \frac{t}{\tau_q}, \quad \theta = \frac{\tau_s}{\tau_q} \quad (11)$$

Note that equation (11) is different from the dimensionless definitions used in *Lin and Yeh* [2017]. The dimensionless governing equation and related conditions for confined flow based on equation (11) are given as

$$(1 + \theta \frac{\partial}{\partial t_D}) (\frac{\partial^2 s_D}{\partial r_D^2} + \frac{1}{r} \frac{\partial s_D}{\partial r_D}) = (1 + \frac{\partial}{\partial t_D}) \frac{\partial s_D}{\partial t_D}, \quad (r_D, t_D) \in [r_{w,D}, \infty) \times (0, \infty) \quad (12)$$

with

$$s_D|_{t_D=0} = \frac{\partial s_D}{\partial t_D} \Big|_{t_D=0} = 0 \quad (13)$$

$$\frac{\partial s_D}{\partial r_D} \Big|_{r_D=r_{w,D}} = -\frac{2}{r_{w,D}} \quad (14)$$

$$\lim_{r_D \rightarrow \infty} s_D = 0 \quad (15)$$

The equations can be solved similar to the work of *Lin and Yeh* [2017], but herein the numerical Laplace inversion will be used to calculate the time-domain value of its solution in the Laplace domain. Later, assuming $r_{w,D} \rightarrow 0$ to eliminate the wellbore radius effect, the Laplace domain solution is

$$\bar{s}_D = \frac{2}{p} K_0(\sqrt{\frac{p+p^2}{1+p\theta}} r_D) \quad (16)$$

where the overbar denotes the function in the Laplace domain, p is the Laplace parameter, and $K_0(\cdot)$ is the second kind of modified Bessel function of zero order. The numerical Laplace inversion scheme will be postponed to the Subsection 3.4 for the detailed introduction.

The default values of Q , T , and S are assumed as 500 m³/h, 10 m²/h, and 1×10^{-4} modified from Table 1 of *Lin and Yeh* [2017]. Apparently, if $\theta = 1$, the lagging effect is negligible and the solution will be reduced to the *Theis* [1935] solution. If θ is zero, the solution becomes an SPL or CV model. In addition, as θ is greater than unit, the solution is the lagging model. Figure 6 demonstrates the dimensionless drawdown versus the dimensionless time with $\theta = 0, 1$, and 10 observed at $r_D = 1$.

245 It can be seen that s_D increases with θ . However, when the value of θ is equal to 0, the drawdown
 246 starts to respond to the pumping well at $t_D = 1$. It is the effect of the inertial force on the movement
 247 of water due to fast pumping that delays the propagation of drawdown. On the other hand, if θ is
 248 greater than unit, the drawdown curves show S-shaped patterns. This is so because dead-end pores or
 249 residual pores play a role in recharging toward the well at intermediate times and causing a flattening
 250 portion. According to this figure, one can say that the inertial force dominates the groundwater flow
 251 when θ is less than a unit, while the recharge of dead end pores prevails in the flow system as $\theta < 1$.

252 3.1.2 Unconfined Flow

253 Herein, a new defined dimensionless parameters are applied to the work of *Lin et al.* [2019].

$$254 \begin{aligned} s_D &= \frac{4\pi K_r b s}{Q}, & r_D &= \frac{r}{\sqrt{K_r \tau_q / S_s}}, & z_D &= \frac{z}{\sqrt{K_r \tau_q / S_s}}, & b_D &= \frac{b}{\sqrt{K_r \tau_q / S_s}}, \\ t_D &= t / \tau_q, & \theta &= \tau_s / \tau_q, & \kappa &= K_z / K_r, & \eta &= \sqrt{\frac{S_y^2 K_r}{K_z^2 S_s \tau_q}}. \end{aligned} \quad (17)$$

254 Then, the governing equation in the aquifer can be expressed as

$$255 \frac{\partial^2 s_D}{\partial r_D^2} + \frac{1}{r} \frac{\partial s_D}{\partial r_D} + \kappa \frac{\partial^2 s_D}{\partial z_D^2} = \frac{\partial s_D}{\partial t_D}, \quad (r_D, z_D) \in (0, \infty) \times [0, b_D] \quad (18)$$

256 where K_r and K_z are hydraulic conductivities [LT^{-1}] in r and z directions, S_s is the specific storage
 257 [L^{-1}], and b is the aquifer thickness [L].

258 The dimensionless initial condition is the same as the equation (13), especially for the water
 259 table. The dimensionless inner boundary condition is

$$\lim_{r_D \rightarrow 0} r_D \frac{\partial s_D}{\partial r_D} = -2 \quad (19)$$

259 The outer boundary has the same form as shown in equation (15).

260 The base of the aquifer is often impermeable (aquiclude). The no-flow condition is imposed on
 261 and that gives a dimensionless form as

$$s_D(z_D = 0) = 0. \quad (20)$$

262 The upper kinematic condition on the water table using lagging theory can be expressed in the
 263 dimensionless form as:

$$(1 + \theta \frac{\partial}{\partial t_D}) \frac{\partial s_D}{\partial z_D} \Big|_{z_D=b_D} = -\eta (1 + \frac{\partial}{\partial t_D}) \frac{\partial s_D}{\partial t_D} \Big|_{z_D=b_D}. \quad (21)$$

264 The above equations can be solved using the Laplace transform method and Hankel transform method.
 265 The detailed derivation is similar to that provided by *Lin et al.* [2019]. The default values used in
 266 the drawdown evaluation are $Q = 1 \times 10^{-3} \text{ m}^3/\text{s}$, $b = 10 \text{ m}$, $K_r = 1 \times 10^{-4} \text{ m/s}$, $K_z = 5 \times 10^{-5} \text{ m/s}$, S_s
 267 $= 1 \times 10^{-4} \text{ m}^{-1}$, and $S_y = 0.2$. The observation point is chosen at $0.99b$, which is close to the water

268 table to highlight the drainage effect. Moreover, these default values are modified from the work of
 269 *Lin et al.* [2019].

270 Figure (7) demonstrates the time-drawdown curves in dimensionless form when θ is equal to 0,
 271 1, and 10. Similar to the results shown in Figure 6, the drawdown increases with θ . For the case of
 272 $\theta = 0$, the water table condition becomes a CV-type condition, which means that fast drainage will
 273 occur at early times. Therefore, the drawdown in the early period is quite small compared to others.
 274 For the case of $\theta = 1$, it is the typical *Neuman* [1972] solution with a slight S-shaped curve. For the
 275 case of $\theta = 10$, the water table is subject to the lagging condition. It exhibits a late drainage, resulting
 276 in the greatest drawdown. One can conclude that when $\theta < 1$, the fast drainage from excess water is
 277 dominated at the capillary fringe. On the other hand, $\theta > 1$ means that capillary suction controls the
 278 drainage rate and slowly releases residual water in the unsaturated zone to the pumping well. This
 279 effect is similar to the condition proposed by *Moench* [1995]—drainage may gradually release from
 280 the vadose zone. In short, judging from the value of θ facilitates in the evaluation of the properties
 281 of the capillary zone.

282 3.1.3 Solving Technique

283 To solve the equations resulting from lagging theory, the Laplace transform method is a very
 284 useful technique to converge t to the Laplace parameter p . However, the solution solved in the Laplace
 285 domain may not be easily transferred to the time domain analytically; thus, the numerical Laplace
 286 transform technique is recommended to evaluate the time-domain value. *Tzou et al.* [1994] provided
 287 a numerical Laplace transform method based on the Riemann sum approximation. It can provide
 288 accurate results if the summation terms are large enough. However, the numerical Laplace inversion
 289 scheme suggested here is called the concentrated matrix-exponential (CME) method proposed by
 290 *Horváth et al.* [2020]. Compared to Euler- or Gaver-based inversions, the CME method has the best
 291 numerical stability, avoids overshooting and undershooting issues, and gains accurate results as the
 292 order used in the CME increases. The authors of *Horváth et al.* [2020] provided the code written in
 293 Mathematica, Matlab, and Python scripts, and the readers can get these codes for free in the GitHub
 294 repository at <https://github.com/ghorvath78/iltcme>. Moreover, the reader can apply the
 295 extending version of the CME method called CME-S *Horváth et al.* [2022], which is more robust
 296 and available by directly contacting the authors of *Horváth et al.* [2022].

297 4 Candidate Mathematical Models using Lagging Theory

298 To choose the possible models to apply the lagging theory, it should be noted that the target
 299 effect should have a profound effect on hydraulic responses, for example, the pumping test, which
 300 focuses particularly on the small drawdown value at the beginning of the onset. Therefore, the
 301 lagging theory in the model can be meaningful. We list three models that may be chosen for the

302 application of lagging theory. Note that we will not solve the equations to make them flexible for
 303 various boundary value problems and coordinate axis.

304 4.1 Candidate Model 1: DP Model

305 The DP model with the first mass transfer rate between the fracture and matrix continua. As
 306 mentioned previously, the *Lin and Yeh* [2017] model was developed to depict flow behavior in
 307 the fractured aquifer system, and it is capable of reflecting an S-shaped time drawdown curve, the
 308 characteristic of the DP media. The difference is that we remain with the governing equations for
 309 the fracture flow and matrix flow, respectively, expressed as

$$S_{s,f} \frac{\partial s_f}{\partial t} = \mathbf{K} \nabla^2 s - q \quad (22)$$

310 and

$$S_{s,m} \frac{\partial s_m}{\partial t} = q \quad (23)$$

311 where the q is the matrix-to-fracture flux. The flux q can be expressed as a first-order mass transfer
 312 term between the drawdowns in fracture and matrix; that gives

$$q = K_m \sigma (s_f - s_m) \quad (24)$$

313 According to the concept of lagging theory, equation (24) can be assumed to occur at different times.
 314

$$q(t + \tau_q) = K_m \sigma (s_f - s_m)|_{t+\tau_s} \quad (25)$$

315 Applying the truncated Taylor series expansion to equation (25), it can be re-expressed as

$$(1 + \tau_q \frac{\partial}{\partial t}) q(t) = (1 + \tau_s \frac{\partial}{\partial t}) K_m \sigma (s_f - s_m)|_t \quad (26)$$

316 Substituting this result into equations (22) and (23), we obtain

$$S_{s,f} \frac{\partial s_f}{\partial t} = \mathbf{K} \nabla^2 s - \frac{(1 + \tau_s \frac{\partial}{\partial t}) K_m \sigma (s_f - s_m)}{1 + \tau_q \frac{\partial}{\partial t}} \quad (27)$$

317 and

$$S_{s,m} \frac{\partial s_m}{\partial t} = \frac{(1 + \tau_s \frac{\partial}{\partial t}) K_m \sigma (s_f - s_m)}{1 + \tau_q \frac{\partial}{\partial t}} \quad (28)$$

318 Apparently, two lagging parameters control the rate of release from the matrix blocks to the fractures.
 319 If τ_q is greater than τ_s , the drawdown gradient is the cause that drives the flux. The channel connected
 320 between the fracture and the matrix may suffer from a fast flow speed that exerts an inertial effect
 321 due to the rapid decline of the drawdown, causing the flow to delay to the aquifer, especially near
 322 the pumping well. On the other hand, when τ_s is greater than τ_q , the channel can contain many
 323 additional pores that store water and recharge to fracture acting as water sources.

4.2 Candidate Model 2: Leaky Aquifer Model

Leaky aquifer, especially the model of *Hantush and Jacob* [1955], is governed by

$$S \frac{\partial s}{\partial t} = T \nabla^2 s - q \quad (29)$$

where S and T are the storativity and transmissivity of the leaky aquifer, respectively, q is the leakage flux of an aquitard and can be defined as

$$q = \beta' (s - 0) \quad (30)$$

where β' is the leakance [T^{-1}] defined as the ratio of the aquitard hydraulic conductivity to aquitard thickness. This equation states that leakage is proportional to the drawdown difference between the aquifer and the constant water table.

Again, using the lagging theory along with the Taylor series expansion to equation (30), reading

$$(1 + \tau_q \frac{\partial}{\partial t})q = (1 + \tau_s \frac{\partial}{\partial t})\beta' s \quad (31)$$

Thence, the governing equation for leaky aquifer, equation (29), can be rewritten as

$$S \frac{\partial s}{\partial t} = T \nabla^2 s - \frac{1 + \tau_s \frac{\partial}{\partial t}}{1 + \tau_q \frac{\partial}{\partial t}} \beta' s \quad (32)$$

Similar to the previous model, τ_q and τ_s may have a similar effect on pump-induced drawdown. When $\tau_q > \tau_s$, the leakage effect would occur earlier compared to expectation, while $\tau_q < \tau_s$ results in a late leakage effect on the hydraulic response. We can expect it to be more flexible in predicting or fitting the drawdown curve due to pumping in a leaky aquifer.

4.3 Candidate Model 3: Unsaturated Flow Model

The pump-induced unconfined flow considering vertical unsaturated flow. Instead of using the water table kinematic condition to mathematically reflect the delayed drainage effect on drawdown in the intermediate stage, several models have been developed that account for the linearized unsaturated flow above the water table by fixing the water table location [*Mathias and Butler*, 2006; *Tartakovsky and Neuman*, 2007; *Mishra and Neuman*, 2010]. Among them, *Tartakovsky and Neuman* [2007] has a much simpler equation for the unsaturated flow. Thus, we use their model as an example. When the lateral flow effect is eliminated, the governing equation describing the vertical unsaturated flow is as follows.

$$S_y \frac{\partial s_u}{\partial t} = K_z \left(\frac{\partial^2 s_u}{\partial z^2} - \kappa \frac{\partial s_u}{\partial z} \right) \quad (33)$$

where the subscript u means the unsaturated zone, z is the vertical direction from the base of the aquifer, and κ is the unsaturated coefficient [L^{-1}].

The continuity requirements at the interface between the unsaturated zone and saturated zone are

$$s_u(z = b) = s(z = b) \quad (34)$$

$$\left. \frac{\partial s_u}{\partial z} \right|_{z=b} = q \quad (35)$$

where b is the aquifer thickness and q is the flux draining into the saturated zone equal to $\partial s / \partial z$.
Employing the lagging theory to this relationship, the flux continuity becomes

$$(1 + \tau_q \frac{\partial}{\partial t})q = (1 + \tau_s \frac{\partial}{\partial t}) \frac{\partial s}{\partial z}, \quad (36)$$

and then replace this result with equation (35), giving

$$\left. \frac{\partial s_u}{\partial z} \right|_{z=b} = \frac{1 + \tau_s \frac{\partial}{\partial t}}{1 + \tau_q \frac{\partial}{\partial t}} \left. \frac{\partial s}{\partial z} \right|_{z=b} \quad (37)$$

Therefore, equation (37) bears the effect of fast and very slow drainage from the unsaturated zone on the aquifer drawdown. Rapid drainage can result from a significantly decreasing water table due to a higher pumping rate, especially in the vicinity of the pumping well, which drives the water from the unsaturated zone at early times. Slow drainage may be the result of capillary suction. The physical interpretation of two lagging parameters here can refer to the work of *Lin et al.* [2019].

5 Discussion, Limitations, and Conclusion

This study reviews five published articles related only to the lagging theory (derived from the DPL concept) although the DPL model has already been widely applied in the fields of thermal engineering. There is no doubt about the similarity between the lagging theory and the DPL theory proposed by *Tzou* [1995]. The term lagging theory is used to distinguish DPL, which focuses on the heat transfer problem. Being the bridge between hydrology and thermal engineering, this paper also provides three candidate directions (i.e., water transfer term in a DP model, aquitard leakage term in *Hantush and Jacob* [1955] leaky aquifer model, and the continuity requirement used in a coupled saturated and unsaturated flow model) to apply the lagging theory to the model for groundwater flow. These models can be solved using the Laplace transform technique, and the reader can assign the boundary condition to any type of problem.

However, the limitation of the lagging theory is that the reliable range of the lagging parameters is not established because of the utter lack of study on lagging theory, namely, only five related studies have been applied to perform the parameter identification. It would be a challenge for hydraulic parameter estimation if both lagging parameters are not well determined from broad experiments. However, the initial guesses of the lag parameters can refer to the ranges provided previously [*Lin and Yeh, 2017; Lin et al., 2019*], and those and the threshold value θ are listed in Table 1. The other challenge is that the lagging parameters could lead to infinite solutions if all estimates are not

375 subject to a proper search range. This will result in an inaccurate prediction for the forward problem.
 376 Fortunately, in most of the study areas, the hydraulic conductivity and the specific storage or specific
 377 yield were determined by conventional solutions. Thus, the objective function for the least squares —
 378 $\sum_{i=1}^N (s^* - s)^2$ — can be rewritten as $\sum_{i=1}^N (s_i^* - s_i)^2 + |K - K_{\text{target}}/l| + |S_s - S_{s,\text{target}}/l| + |S_y - S_{y,\text{target}}/l|$,
 379 where s_i^* is the drawdown measured at the i -th time, K_{target} , $S_{s,\text{target}}$, and $S_{y,\text{target}}$ are known estimates
 380 from previous aquifer tests, and l is a scale factor and suggested as 50 or other values. Such a
 381 treatment guides the optimization method to seek the smallest solution near the previous determined
 382 parameters and avoid the infinite solutions or trap into a local minimal.

383 Overall, lagging theory, like the DPL model, has a huge potential for hydrologists to develop
 384 their models. The benefit of using two additional parameters is not only to describe the flow for a
 385 better fit to the data, but the lagging time parameters also convey some information from the study
 386 area, such as fast or slow drainage/water exchange rate. It helps to know more about the hidden
 387 processes under the aquifer and to develop a strategy for managing water resources.

388 Acknowledgments

389 Many thanks to Prof. Robert Tzou, who made a great contribution to the DPL studies, for encouraging
 390 me to do this research and providing constructional comments on this article to improve the quality of
 391 the article. The authors also thank Dr. Dudley Benton for his practical suggestions on the parameter
 392 identification and his encouragement.

393 References

- 394 Bevan, M. J., A. L. Endres, D. L. Rudolph, and G. Parkin (2005), A field scale study of pumping-
 395 induced drainage and recovery in an unconfined aquifer, *Journal of Hydrology*, 315(1-4), 52–70,
 396 doi:<https://doi.org/10.1016/j.jhydrol.2005.04.006>.
- 397 Boulton, N. (1954a), Unsteady radial flow to a pumped well allowing for delayed yield from storage,
 398 *Int. Assoc. Sci. Hydrol. Publ.*, 2, 472–477.
- 399 Boulton, N. S. (1954b), The drawdown of the water-table under non-steady conditions near a pumped
 400 well in an unconfined formation., *Proceedings of the Institution of Civil Engineers*, 3(4), 564–579,
 401 doi:<https://doi.org/10.1680/ipeds.1954.12586>.
- 402 Cattaneo, C. (1958), A form of heat-conduction equations which eliminates the paradox of instantane-
 403 ous propagation, *Comptes Rendus*, 247, 431.
- 404 Chaudhry, A. (2003), *Gas well testing handbook*, Gulf professional publishing.
- 405 Greene, E. A. (1993), *Hydraulic properties of the Madison aquifer system in the western Rapid City*
 406 *area, South Dakota*, vol. 93, US Department of the Interior, US Geological Survey.
- 407 Hantush, M. S., and C. E. Jacob (1955), Non-steady radial flow in an infinite leaky aquifer,
 408 *Eos, Transactions American Geophysical Union*, 36(1), 95–100, doi:<https://doi.org/10.1029/>

- 409 TR036i001p00095.
- 410 Horváth, G., I. Horváth, S. A.-D. Almousa, and M. Telek (2020), Numerical inverse laplace trans-
 411 formation using concentrated matrix exponential distributions, *Performance Evaluation*, 137,
 412 102,067, doi:<https://doi.org/10.1016/j.peva.2019.102067>.
- 413 Horváth, I., A. Mészáros, and M. Telek (2022), Numerical inverse laplace transformation beyond
 414 the abate–whitt framework, *Journal of Computational and Applied Mathematics*, p. 114651,
 415 doi:<https://doi.org/10.1016/j.cam.2022.114651>.
- 416 Huang, C.-S., Z. Wang, Y.-C. Lin, H.-D. Yeh, and T. Yang (2020), New analytical models for flow
 417 induced by pumping in a stream-aquifer system: A new robin boundary condition reflecting joint
 418 effect of streambed width and storage, *Water Resources Research*, 56(4), e2019WR026,352.
- 419 Hunt, B. (1999), Unsteady stream depletion from ground water pumping, *Groundwater*, 37(1),
 420 98–102, doi:<https://doi.org/10.1111/j.1745-6584.1999.tb00962.x>.
- 421 Lin, Y.-C., and H.-D. Yeh (2017), A lagging model for describing drawdown induced by a constant-
 422 rate pumping in a leaky confined aquifer, *Water Resources Research*, 53(10), 8500–8511, doi:
 423 <https://doi.org/10.1002/2017WR021115>.
- 424 Lin, Y.-C., C.-S. Huang, and H.-D. Yeh (2019), Analysis of unconfined flow induced by constant
 425 rate pumping based on the lagging theory, *Water Resources Research*, 55(5), 3925–3940, doi:
 426 <https://doi.org/10.1029/2018WR023893>.
- 427 Löfqvist, T., and G. Rehbinder (1993), Transient flow towards a well in an aquifer including the
 428 effect of fluid inertia, *Applied scientific research*, 51(3), 611–623, doi:[https://doi.org/10.1007/](https://doi.org/10.1007/BF00868003)
 429 BF00868003.
- 430 Malama, B. (2011), Alternative linearization of water table kinematic condition for unconfined
 431 aquifer pumping test modeling and its implications for specific yield estimates, *Journal of hydrology*,
 432 399(3-4), 141–147, doi:<https://doi.org/10.1016/j.jhydrol.2010.11.007>.
- 433 Mathias, S., and A. Butler (2006), Linearized richards’ equation approach to pumping test anal-
 434 ysis in compressible aquifers, *Water resources research*, 42(6), doi:[https://doi.org/10.1029/](https://doi.org/10.1029/2005WR004680)
 435 2005WR004680.
- 436 Mishra, P. K., and S. P. Neuman (2010), Improved forward and inverse analyses of saturated-
 437 unsaturated flow toward a well in a compressible unconfined aquifer, *Water Resources Research*,
 438 46(7), doi:<https://doi.org/10.1029/2009WR008899>.
- 439 Moench, A. F. (1995), Combining the neuman and boulton models for flow to a well in an unconfined
 440 aquifer, *Groundwater*, 33(3), 378–384, doi:<https://doi.org/10.1111/j.1745-6584.1995.tb00293.x>.
- 441 Moench, A. F., S. P. Garabedian, and D. R. LeBlanc (2000), Estimation of hydraulic parameters
 442 from an unconfined aquifer test conducted in a glacial outwash deposit, cape cod, massachusetts,
 443 *Tech. rep.*, GERON CORP MENLO PARK CA.

- 444 Neuman, S. P. (1972), Theory of flow in unconfined aquifers considering delayed response
445 of the water table, *Water Resources Research*, 8(4), 1031–1045, doi:[https://doi.org/10.1029/
446 WR008i004p01031](https://doi.org/10.1029/WR008i004p01031).
- 447 Neuman, S. P. (1974), Effect of partial penetration on flow in unconfined aquifers considering
448 delayed gravity response, *Water resources research*, 10(2), 303–312, doi:[https://doi.org/10.1029/
449 WR010i002p00303](https://doi.org/10.1029/WR010i002p00303).
- 450 Neuman, S. P. (1975a), Analysis of pumping test data from anisotropic unconfined aquifers
451 considering delayed gravity response, *Water Resources Research*, 11(2), 329–342, doi:[https://doi.org/10.1029/
452 //doi.org/10.1029/WR011i002p00329](https://doi.org/10.1029/WR011i002p00329).
- 453 Neuman, S. P. (1975b), Analysis of pumping test data from anisotropic unconfined aquifers
454 considering delayed gravity response, *Water Resources Research*, 11(2), 329–342, doi:[https://doi.org/10.1029/
455 //doi.org/10.1029/WR011i002p00329](https://doi.org/10.1029/WR011i002p00329).
- 456 Nwankwor, G., R. Gillham, G. van der Kamp, and F. Akindunni (1992), Unsaturated and saturated
457 flow in response to pumping of an unconfined aquifer: Field evidence of delayed drainage,
458 *Groundwater*, 30(5), 690–700, doi:<https://doi.org/10.1111/j.1745-6584.1992.tb01555.x>.
- 459 Pascal, H. (1986), Pressure wave propagation in a fluid flowing through a porous medium and
460 problems related to interpretation of stoneley's wave attenuation in acoustical well logging,
461 *International Journal of Engineering Science*, 24(9), 1553–1570, doi:[https://doi.org/10.1016/
462 0020-7225\(86\)90163-1](https://doi.org/10.1016/0020-7225(86)90163-1).
- 463 Sarmah, R., I. Sonkar, and S. R. Chavan (2022), Analytical solutions for predicting seepage in a
464 layered ditch drainage system under dirichlet and lagging robin boundary conditions, *Hydrological
465 Sciences Journal*, (just-accepted), doi:<https://doi.org/10.1080/02626667.2022.2101891>.
- 466 Sophocleous, M., A. Koussis, J. Martin, and S. Perkins (1995), Evaluation of simplified stream-
467 aquifer depletion models for water rights administration, *Groundwater*, 33(4), 579–588, doi:
468 <https://doi.org/10.1111/j.1745-6584.1995.tb00313.x>.
- 469 Spalding, C. P., and R. Khaleel (1991), An evaluation of analytical solutions to estimate drawdowns
470 and stream depletions by wells, *Water Resources Research*, 27(4), 597–609, doi:[https://doi.org/
471 10.1029/91WR00001](https://doi.org/10.1029/91WR00001).
- 472 Sun, D., and H. Zhan (2007), Pumping induced depletion from two streams, *Advances in Water
473 Resources*, 30(4), 1016–1026, doi:<https://doi.org/10.1016/j.advwatres.2006.09.001>.
- 474 Tartakovsky, G. D., and S. P. Neuman (2007), Three-dimensional saturated-unsaturated flow with ax-
475 ial symmetry to a partially penetrating well in a compressible unconfined aquifer, *Water Resources
476 Research*, 43(1), doi:<https://doi.org/10.1029/2006WR005153>.
- 477 Theis, C. V. (1935), The relation between the lowering of the piezometric surface and the rate
478 and duration of discharge of a well using ground-water storage, *Eos, Transactions American
479 Geophysical Union*, 16(2), 519–524, doi:<https://doi.org/10.1029/TR016i002p00519>.

- 480 Tzou, D., M. Özisik, and R. Chiffelle (1994), The lattice temperature in the microscopic two-step
481 model, doi:<https://doi.org/10.1115/1.2911439>.
- 482 Tzou, D. Y. (1995), The generalized lagging response in small-scale and high-rate heating, *Inter-*
483 *national Journal of Heat and Mass Transfer*, 38(17), 3231–3240, doi:[https://doi.org/10.1016/](https://doi.org/10.1016/0017-9310(95)00052-B)
484 0017-9310(95)00052-B.
- 485 Tzou, D. Y. (2014), *Macro-to microscale heat transfer: the lagging behavior*, John Wiley & Sons.
- 486 Vernotte, P. (1958), Les paradoxes de la theorie continue de l'equation de la chaleur, *Comptes rendus*,
487 246, 3154.
- 488 Vernotte, P. (1961), Some possible complications in the phenomena of thermal conduction, *Compte*
489 *Rendus*, 252(1), 2190–2191.
- 490 Warren, J., and P. J. Root (1963), The behavior of naturally fractured reservoirs, *Society of Petroleum*
491 *Engineers Journal*, 3(03), 245–255, doi:<https://doi.org/10.2118/426-PA>.
- 492 Xiong, M., C. Tong, and C.-S. Huang (2021), A new approach to three-dimensional flow in a pumped
493 confined aquifer connected to a shallow stream: Near-stream and far-from-stream groundwater
494 extractions, *Water Resources Research*, 57(4), e2020WR028,780.

495 **Acronyms**

	CME	Concentrated matrix-exponential,
	CV	Cattaneo-Vernotte,
496	DP	Dual porosity,
	DPL	Dual-phase lag,
	SPL	Single-phase lag.

Table 1. Possible range for lagging parameters τ_q and τ_s

Parameters	Minimal value (hour)	Maximal value (hour)	Note
Fractured aquifer ^[1]			
τ_q	0.09	13.92	–
τ_s	0.05	7.12	–
θ	0.56	0.51	Inertial force dominates
Unconfined aquifer ^[2]			
τ_q	0.67	194.37	–
τ_s	30.37	469.40	–
θ ^[3]	45.33	2.42	Capillary suction dominates

¹ The estimates are from the study of *Lin and Yeh* [2017] for fractured aquifer.

² The estimates are from that of *Lin et al.* [2019] for unconfined aquifer.

³ The parameter θ is threshold value defined as τ_s/τ_q [Tzou, 1995].

498 **Figure Captions**

499 **Figure 1.** Word cloud of searching the key word of “dual phase lag” using Google Scholar.

500 **Figure 2.** The lagging response induced by pumping in a porous medium for the cases of (a) $\tau_s > \tau_q$, (b)
501 $\tau_s < \tau_q$, and (c) $\tau_q = \tau_s = 0$. (modified from the figure in Chapter 2 in Tzou [2014]).

502 **Figure 3.** Schematic diagram of fractures with inertia and dead-end pores.

503 **Figure 4.** Schematic diagram of pump-induced unconfined aquifer with quick and slow drainage.

504 **Figure 5.** Temporal drawdown responses due to withdrawal the river through a streambed predicted by DPL
505 and SPL concept with various values of τ_q and τ_s subject to $\tau_q - \tau_s = 1$ h.

506 **Figure 6.** Temporal dimensionless drawdown responses with various values of θ for confined flow.

507 **Figure 7.** Temporal dimensionless drawdown responses with various values of θ for unconfined flow.